HHS Public Access

Author manuscript

*ACS Infect Dis*. Author manuscript; available in PMC 2020 November 17.

Published in final edited form as:

*ACS Infect Dis*. 2020 November 13; 6(11): 3083–3088. doi:10.1021/acsinfecdis.0c00594.

# Antimicrobial Synergy of a Ribonuclease and a Peptide Secreted by Human Cells

**Chelcie H. Eller**[†], **Ronald T. Raines**[*,†,‡,§]

[†]Department of Biochemistry, University of Wisconsin–Madison, Madison, Wisconsin 53706, United States;

[‡]Department of Chemistry, University of Wisconsin–Madison, Madison, Wisconsin 53706, United States;

[§]Department of Chemistry, Massachusetts Institute of Technology, Cambridge, Massachusetts 02139, United States

## Abstract

LL-37 is a secretory peptide that has antimicrobial activity. Ribonuclease 1 (RNase 1) is a secretory enzyme that is not cytotoxic. We find that human LL-37 and human RNase 1 can act synergistically to kill Gram-negative bacterial cells. In the presence of nontoxic concentrations of LL-37, RNase 1 is toxic to *Escherichia coli* cells at picomolar levels. Using wild-type RNase 1 and an inactive variant labeled with a fluorophore, we observe the adherence of RNase 1 to *E. coli* cells and its cellular entry in the presence of LL-37. These data suggest a natural means of modulating the human microbiome via the cooperation of an endogenous peptide (37 residues) and small enzyme (128 residues).

## Graphical Abstract

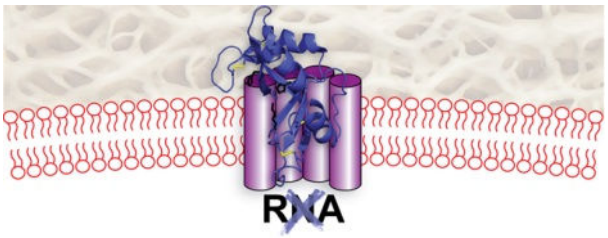


### Keywords

antimicrobial peptide; cathelicidin; microbiome; ribonuclease 1; synergism

[*]**Corresponding Author: Ronald T. Raines** – Department of Biochemistry and Department of Chemistry, University of Wisconsin–Madison, Madison, Wisconsin 53706, United States; Department of Chemistry, Massachusetts Institute of Technology, Cambridge, Massachusetts 02139, United States; rtraines@mit.edu.

Accession Code

Human RNase 1 P07998.

The authors declare no competing financial interest.

Skin is the largest organ in humans. While covering ~18 square feet of our bodies,[1] human skin harbors a large and complex microbiome.[2] This ecosystem is modulated by the cutaneous innate and adaptive immune responses.[3] A prominent modulatory role is played by two distinct families of antimicrobial peptides: defensins and cathelicidins.[4–11] Humans have 10 defensins but only 1 cathelicidin: LL-37.[12,13] This 37-residue cationic peptide, which has two N-terminal leucine ("L") residues, forms a pore in microbial membranes to invoke its toxic activity.[14,15] LL-37 is secreted from epithelial and other cells, and is found in several bodily fluids, including plasma, mucosa, breast milk, and seminal fluid.[16]

In addition to secreting antimicrobial peptides, human cells secrete at least eight homologous ribonucleases, RNases 1–8, each expressed from a gene located on chromosome 14q11.2.[17,18] Of these homologues, RNase 1 (UniProtKB P07998) is the best characterized and most abundant. The expression of the *RNASE1* gene is widespread,[19] and RNase 1 is present in sera at ~0.5 μg/mL (~30 nM).[20] This small (14.6 kDa) enzyme is a highly efficient catalyst of RNA cleavage ($k_{cat}/K_M = 2.8 \times 10^6$ $M^{-1}s^{-1}$)[21] and a well-known scourge in molecular biology and clinical chemistry laboratories.[22,23]

RNase 1 has been implicated in physiological processes.[17,24,25] Human endothelial cells release stored RNase 1 when stimulated with viral RNA agonists of Toll-like receptors.[21] Its addition to dendritic immune cells stimulates the secretion of cytokines.[26] RNase 1 degrades extracellular RNA, which is a natural procoagulant,[27] and the plasma of RNase 1 knockout (*Rnase1*$^{-/-}$) mice clots more rapidly than does wild-type plasma.[28] An engineered variant of RNase 1 that evades a cytosolic inhibitor protein[29,30] exhibits specific toxicity for cancer cells and is in clinical trials as a chemotherapeutic agent.[31,32] RNase 1 also has demonstrable antiviral activity.[25,33] Nevertheless, RNase 1 is not known to have antimicrobial activity.[18]

RNase 1 gains access to RNA within human cells after binding to the glycocalyx, undergoing endocytosis, and translocating to the cytosol.[34,35] We reasoned that microbial cells resist the toxicity of RNase 1 by being impenetrable to the enzyme. Given that LL-37 forms a pore in microbial membranes,[14,15] we suspected that these two denizens of human skin could act in concert to elicit antimicrobial activity. Our findings unveil a natural strategy for modulating the human microbiome.

## RESULTS

### Production of Proteins and Peptides.

Human RNase 1 and its H12A, P19C, and H12A/P19C variants were produced by heterologous expression in *E. coli*. The H12A substitution excises a key active-site imidazoyl group and thus obviates ribonucleolytic activity.[21,30,36,37] In contrast, the P19C substitution is inconsequential to the structure and function of RNase 1[38–40] but provides a sulfhydryl group for the site-specific conjugation of a BODIPY dye to generate RNase 1–BODIPY or H12A RNase 1–BODIPY.

Human LL-37 and Cys–LL-37 were prepared by chemical synthesis. The added N-terminal cysteine of Cys–LL-37 provides a site for the conjugation of a rhodamine dye to generate LL-37–rhodamine without compromising function.[15]

### Antimicrobial Synergy of RNase 1 and LL-37.

*Escherichia coli* was chosen as a representative bacterium in this initial study. Under our conditions, we found that LL-37 has a minimum inhibitory concentration (MIC) against *E. coli* of 8.9 μM, that is, 40 μg/mL (Figure 1). This value is similar to those that were determined previously.[41,42] No growth inhibition was observed at LL-37 concentrations that were ≤1.7 μM.

In contrast to LL-37, the treatment of *E. coli* cells with RNase 1 did not lead to observable toxicity, even at a concentration of 50 μM (Figure 2). Thus, RNase 1 alone is unlikely to be consequential for *E. coli* in humans.

Remarkably, treating *E. coli* cells with sub-MIC concentrations of LL-37 and concentrations of RNase 1 in the picomolar range halted bacterial growth (Figure 2). This synergistic antimicrobial effect is dependent on ribonucleolytic activity, as treating *E. coli* with LL-37 plus H12A RNase 1 did not lead to toxicity (Figure 2).

### Toxicity of RNase 1 and LL-37 for Human Cells.

The cytotoxic synergy of RNase 1 and LL-37 does not extend to human cells. Erythrocytes (that is, red blood cells) do not contain RNA and thus should not be vulnerable to a catalyst of RNA cleavage. They could, however, succumb to agents that disrupt the plasma membrane. Indeed, high concentrations of LL-37 are known to exhibit some toxicity towards human cells.[44] We found that human erythrocytes were indeed susceptible to LL-37. The addition of RNase 1 did not, however, increase that susceptibility (Figure 3A). Likewise, human endothelial cells (HUVEC) were susceptible to LL-37, but their susceptibility was not increased by RNase 1 (Figure 3B).

### Binding of RNase 1 and LL-37 to Bacterial Cells.

We suspected that the antimicrobial activity of RNase 1 requires an affinity for the microbial cell surface. Initially, we probed for binding to the cell surface with a “pull-down” assay. In brief, we incubated fluorescently labeled RNase 1 with *E. coli* cells. We used centrifugation to isolate *E. coli* cells and gel electrophoresis to detect RNase 1–BODIPY that had associated with the cells. The results indicated that RNase 1 does have an affinity for *E. coli* cells (Figure 4A). To obtain quantitative data, we employed fluorescence polarization to titrate RNase 1–BODIPY with *E. coli* cells. Again, the results were consistent with an ability of RNase 1 to bind to *E. coli* cells (Figure 4B). The data indicated that each *E. coli* cell binds 50 nM($N_A/K_d$) = $8 \times 10^4$ RNase 1–BODIPY molecules at the midpoint of the titration.

### Internalization of RNase 1 into Bacterial Cells.

The antimicrobial activity of picomolar concentrations of RNase 1 in the presence of LL-37 suggested to us that the enzyme could enter *E. coli* cells via pores formed by LL-37 in the membrane.[14,15] We tested this hypothesis by using fluorescently labeled H12A RNase 1,

which lacks the ribonucleolytic activity necessary for cytotoxicity. Confocal microscopy of single *E. coli* cells showed that H12A RNase 1–rhodamine can enter *E. coli* cells in the presence of LL-37–BODIPY (Figures 5, inset). Flow cytometry confirmed this colocalization and indicated that increasing the concentration of LL-37–BODIPY led to a greater uptake of RNase 1–rhodamine (Figure 5).

## DISCUSSION

Antimicrobial agents can interact synergistically. Typically, this synergy arises from a combination of different cytotoxic strategies. For example, host-defense and other natural peptides can facilitate the access of antibiotic agents to intracellular targets.[41,45–48] We have discovered that a well-known human secretory enzyme and a well-known human secretory peptide display extraordinary antimicrobial activity when used in combination. Even though RNase 1 is benign at 50 μM, femtomolar levels of RNase 1 in combination with sublethal concentrations of LL-37 are intolerable to *E. coli* cells (Figure 2).

A putative mechanism for the synergistic antimicrobial activity of RNase 1 and LL-37 is evident. LL-37 is known to create pores in the membranes of bacterial cells.[14,15] RNase 1 adheres to microbial cells (Figure 4) and is thus poised to enter, given a means to do so. Pores created by LL-37 could provide that means, together with intrinsic gaps in the peptidoglycan layer.[49,50] Unlike RNA in the human cytosol, which contains a ribonuclease inhibitor protein,[29,30] microbial RNA has no known defense against the lethal catalytic activity of an invading ribonuclease. Accordingly, the synergy that we observed could extend to other pore-forming peptides, including defensins.[4–11]

A specific interaction between RNase 1 and LL-37 is not required for their synergistic cytotoxicity. The protein and peptide do not appear to colocalize in *E. coli* cells (Figure 5). The lack of a significant interaction is not surprising, as both RNase 1 and LL-37 are highly cationic, each having a net charge of $Z = +6$. Indeed, we found no evidence for an interaction of LL-37 and RNase 1 by using fluorescence polarization (data not shown).

RNase 1 is known to interact with anionic mammalian glycans such as heparan sulfate and chondroitin sulfate.[21,34,35,51] In contrast, its affinity for bacterial glycans is unknown. We note, however, that an RNase 1 homologue has been shown to associate with lipopolysaccharides, which pave the outer membrane of Gram-negative bacteria such as *E. coli*.[52]

Without the implementation of new antimicrobial approaches, infections are expected to cause 10 million deaths annually by 2050.[53] Our data indicate that RNase 1 and LL-37 could provide an unappreciated first line of defense against bacterial pathogens. Work to explore the implications of this new-found synergism and exploit its utility is ongoing in our laboratory.

## METHODS

### General.

Commercial chemicals and biochemicals were of reagent grade or better, and were used without further purification. Measurements of UV–vis absorption were made with an Infinite® M1000 PRO plate reader from Tecan (Männedorf, Switzerland). All procedures were performed at ambient temperature (~22 °C) and pressure (1.0 atm) unless otherwise specified.

### Preparation of Peptides, Proteins, and Their Conjugates.

LL-37, which has the amino acid sequence LLGDFFRKSKEKIGKEFKRIVQRIKDFLRNLVPRTES ($M_r$ 4493.3), and Cys–LL-37 (which contains an additional N-terminal cysteine residue) were synthesized by Biomatik (Wilmington, DE). Cys–LL-37 was conjugated to BODIPY® FL *N*-(2-aminoethyl)maleimide from Thermo Fisher Scientific (Waltham, MA) and purified by passage through a desalting column from GE Healthcare (Chicago, IL).

RNase 1 and its H12A, P19C, and H12A/P19C variants were produced in *E. coli* and purified as described previously.[51] H12A/P19C RNase 1 was conjugated to rhodamine red $C_2$ maleimide from Thermo Fisher Scientific, and P19C RNase 1 was conjugated to BODIPY FL *N*-(2-aminoethyl)maleimide. The resulting conjugates were purified by cation-exchange chromatography.

### Toxicity for *E. coli* Cells.

A saturated culture of *E. coli* strain RP437[54] in Luria–Bertani medium[55] was diluted by 10000-fold with medium. The diluted cell stock (200 μL/well) was added to the wells of a 96-well round-bottomed plate from Evergreen Scientific (Vernon, CA). A solution of LL-37 or RNase 1 in phosphate-buffered saline (PBS) was then added to the wells in a serial dilution. In all assays, *E. coli* cells were allowed to grow for 18 h at 37 °C with gentle shaking. Cells were counted by measuring the OD at 600 nm. The fraction of viable cells was determined by normalizing with wells treated with PBS (100%) and cells treated with chloramphenicol (0%). Data with LL-37 alone (Figure 1) and RNase 1 alone (Figure 2) were collected from three independent assays, with each being collected in duplicate ($n = 6$). Values are the mean ± SEM. Data with mixtures of LL-37 and RNase 1 (Figure 2) are representative of checkerboard assays ($n = 4$).

### Toxicity for Human Erythrocytes.

Deidentified human erythrocytes were product SER-PRBC from ZenBio (Research Triangle Park, NC). Cells (2% v/v) were washed three times with Tris-buffered saline (0.01 M Tris–HCl, pH 7.2, containing 0.155 M NaCl) by centrifugation at 3500 rpm. The cells were diluted to 1% in a 96-well plate. Increasing concentrations of LL-37, RNase 1, and solutions of LL-37 in the presence of RNase 1 (500 nM) were added to a final volume of 100 μL, and the plate was incubated at 37 °C for 1 h. The plate was then subjected to centrifugation at 4000 rpm for 5 min. The supernatant (80 μL) was transferred to a new plate, and the absorbance of hemoglobin, which is released upon hemolysis, was recorded at 405 nm. The

cell viability was normalized to cells treated with buffer (100%) or Triton X-100 to 4 μg/mL (0%). Data were collected from three independent assays, with each being performed in duplicate ($n = 6$).

### Toxicity for Human Endothelial Cells.

HUVEC cells were product CRL-1730 from the American Type Culture Collection (Manassas, VA). Cells were plated at 5000 cells/well in Dulbecco's modified Eagle's medium (DMEM) from Invitrogen (Carlsbad, CA). After allowing for surface adhesion overnight, cells were treated with LL-37, RNase 1, or H12A RNase 1 as described above for erythrocytes. After 24 h at 37 °C with 5% $CO_2$, the medium was removed and replaced with 60 μL of Cell Titer assay solution from Promega (Fitchburg, WI) diluted 1:5 in DMEM. After a 2 h incubation, the reduction of the tetrazolium dye was measured at 490 nm. The fraction of cells that were metabolically active was calculated by normalizing with cells treated with PBS (100%) or $H_2O_2$ to 200 μM (0%). Data were collected from three independent assays, with each being performed in duplicate ($n = 6$).

### Microbial Cell Binding by Pull-Down.

Microbial binding was assessed by incubating an aliquot (300 μL) of a culture of *E. coli* cells grown to OD ~0.8 with a solution (10 μL) of RNase 1–BODIPY (final concentration: 1 μM) in 20 mM Tris–HCl buffer, pH 7.2, containing NaCl (50 mM). After a 30 min incubation at 37 °C, cells were pelleted by centrifugation, the supernatant was collected, and the pellet was washed with the buffer. The supernatant and pellet were analyzed with SDS–PAGE. RNase 1–BODIPY was imaged by fluorescence using excitation at 470 nm and emission at 530 nm. Total protein was visualized by staining with Coomassie Brilliant Blue G-250 dye.

### Microbial Cell Binding by Fluorescence Polarization.

Fluorescence polarization was employed to assess the affinity of RNase 1 for *E. coli* cells. RNase 1–BODIPY (final concentration: 50 nM) was added to solutions of 20 mM Tris–HCl buffer, pH 7.2, containing NaCl (50 mM) and varied concentrations of bacterial cells. Values of OD at 600 nm were converted to cells/mL by assuming that a solution with $OD_{600\ nm} = 1.0$ contains $8 \times 10^8$ cells/mL. After incubation at 37 °C for 30 min, the luorescence polarization was measured by using excitation at 470 nm and emission at 530 nm. Polarization values were fitted by nonlinear regression analysis to the equation

$$Y = \frac{B_{max}[\text{RNase}]^h}{\left(K_d{}^h + [\text{RNase}]^h\right)}$$

where $Y$ is the relative fluorescence, $B_{max}$ is the maximum relative fluorescence, and $h$ is the Hill coefficient. Assays were performed in triplicate. Data were collected from five independent assays, with each being performed in duplicate ($n = 10$).

### Cellular Internalization of Protein and Peptide.

For cytometry, overnight growths of *E. coli* were diluted with medium until reaching $OD_{600\ nm}$ = 1.0. Cells from a 100 μL aliquot of the diluted cell stock were collected by centrifugation at 3000 rpm for 4 min and washed with PBS. Cells were resuspended in PBS and treated with H12A RNase 1–rhodamine (2.5 μM) and LL-37–BODIPY (2.5 μM). After a 2 h incubation, cells were washed (three times) with PBS and collected by centrifugation. Protein internalization was measured with an LSR Fortessa flow cytometer from BD Biosciences (San Jose, CA) at the University of Wisconsin–Madison Flow Cytometry Laboratory.

For visualization, cells (again, a 100 μL aliquot with $OD_{600\ nm}$ = 1.0) were treated with H12A RNase 1–rhodamine (2.5 μM) and LL-37–BODIPY (2.5 μM), and the mixture was diluted 4-fold with PBS. An aliquot (2.5 μL) of the resulting solution was spotted between agarose (3% w/v) pads on 24 × 50 mm coverslips from Thermo Fisher Scientific. Cells were imaged with an Eclipse Ti laser–scanning confocal microscope from Nikon (Tokyo, Japan) equipped with an Axio Camdigital camera from Carl Zeiss (Oberkochen, Germany).

## ACKNOWLEDGMENTS

We thank Prof. B. Weisblum (University of Wisconsin-Madison) for help with hemolysis assays, Prof. D. B. Weibel (University of Wisconsin-Madison) for the use of his confocal microscope, and Dr. K. J. Hetrick (Massachusetts Institute of Technology) for comments on the manuscript. This work was supported by grant R01 CA073808 (NIH). The University of Wisconsin-Madison Flow Cytometry Laboratory was supported by grant S10 OD018202.

## ABBREVIATIONS

| | |
|---|---|
| **BODIPY** | 4,4-difluoro-4-bora-3a,4a-diaza-*s*-indacene |
| **MIC** | minimum inhibitory concentration |
| **$N_A$** | Avogadro's number |
| **OD** | optical density |
| **PBS** | phosphate-buffered saline |
| **RFU** | relative fluorescence units |
| **RNase** | ribonuclease |
| **SDS–PAGE** | polyacrylamide gel electrophoresis performed in the presence of sodium dodecyl sulfate |
| **Tris** | tris(hydroxymethyl)aminomethane |
| ***Z*** | net charge = Arg + Lys − Asp − Glu |

## REFERENCES

(1). Schmidt C Out of your skin. Nat. Biotechnol 2020, 38, 392–397.

(2). Byrd AL; Beklaid Y; Segre JA The human skin microbiome. Nat. Rev. Microbiol 2018, 16, 143–155. [PubMed: 29332945]

(3). Belkaid Y; Serge JA Dialogue between skin microbiota and immunity. Science 2014, 346, 954–959. [PubMed: 25414304]

(4). Wiesner J; Vilcinskas A Antimicrobial peptides: The ancient arm of the human immune system. Virulence 2010, 1, 440–464. [PubMed: 21178486]

(5). Cederlund A; Gudmundsson GH; Agerberth B Antimicrobial peptides important in innate immunity. FEBS J. 2011, 278, 3942–3951. [PubMed: 21848912]

(6). Pasupuleti M; Schmidtchen A; Malmsten M Antimicrobial peptides: Key components of the innate immune system. Crit. Rev. Biotechnol 2012, 32, 143–171. [PubMed: 22074402]

(7). Mahlapuu M; Håkansson J; Ringstad L; Björn C Antimicrobial peptides: An emerging category of therapeutic agents. Front. Cell. Infect Microbiol 2016, 6, 194. [PubMed: 28083516]

(8). Lei J; Sun L; Huang S; Zhu C; Li P; He J; Mackey V; Coy DH; He Q The antimicrobial peptides and their potential clinical applications. Am. J. Transl. Res 2019, 11, 3919–3931. [PubMed: 31396309]

(9). Mookherjee N; Anderson MA; Haagsman HP; Davidson DJ Antimicrobial host defence peptides: Functions and clinical potential. Nat. Rev. Drug Discovery 2020, 19, 311–332. [PubMed: 32107480]

(10). Magana M; Pushpanathan M; Santos AL; Leanse L; Fernandez M; Ioannidis A; Giulianotti MA; Apidianakis Y; Bradfute S; Ferguson AL; Cherkasov A; Seleem MN; Pinilla C; de la Fuente-Nunez C; Lazaridis T; Dai T; Houghten RA; Hancock REW; Tegos GP The value of antimicrobial peptides in the age of resistance. Lancet Infect. Dis 2020, 20, e216–e230. [PubMed: 32653070]

(11). Lazzaro BP; Zasloff M; Rolff J Antimicrobial peptides: Application informed by evolution. Science 2020, 368, eaau5480. [PubMed: 32355003]

(12). Vandamme D; Landuyt B; Luyten W; Schoofs L A comprehensive summary of LL-37, the factotum human cathelicidin peptide. Cell. Immunol 2012, 280, 22–35. [PubMed: 23246832]

(13). Kahlenberg JM; Kaplan MJ Little peptide, big effects: The role of LL-37 in inflammation and autoimmune disease. J. Immunol 2013, 191, 4895–4901. [PubMed: 24185823]

(14). Lee C-C; Sun Y; Chen CW; Qian S; Huang HW Transmembrane pores formed by human antimicrobial peptide LL-37. Biophys. J 2011, 100, 1688–1696. [PubMed: 21463582]

(15). Li Y; Qian Z; Ma L; Hu S; Nong D; Xu C; Ye F; Lu Y; Wei G; Li M Single-molecule visualization of dynamic transitions of pore-forming peptides among multiple transmembrane positions. Nat. Commun 2016, 7, 12906. [PubMed: 27686409]

(16). Durr UH; Sudheendra US; Ramamoorthy A LL-37, the only human member of the cathelicidin family of antimicrobial peptides. Biochim. Biophys. Acta, Biomembr 2006, 1758, 1408–1425.

(17). Sorrentino S The eight human “canonical” ribonucleases: Molecular diversity, catalytic properties, and special biological actions of the enzyme proteins. FEBS Lett. 2010, 584, 2194–2200. [PubMed: 20388512]

(18). Schwartz L; Cohen A; Thomas J; Spencer JD The immunomodulatory and antimicrobial properties of the vertebrate ribonuclease A superfamily. Vaccines 2018, 6, 76.

(19). Su AI; Wiltshire T; Batalov S; Lapp H; Ching KA; Block D; Zhang J; Soden R; Hayakawa M; Kreiman G; Cooke MP; Walker JR; Hogenesch JB A gene atlas of the mouse and human protein-encoding transcriptomes. Proc. Natl. Acad. Sci. U. S. A 2004, 101, 6062–6067. [PubMed: 15075390]

(20). Weickmann JL; Olson EM; Glitz DG Immunological assay of pancreatic ribonuclease in serum as an indicator of pancreatic cancer. Cancer Res. 1984, 44, 1682–1687. [PubMed: 6704974]

(21). Eller CH; Lomax JE; Raines RT Bovine brain ribonuclease is the functional homolog of human ribonuclease 1. J. Biol. Chem 2014, 289, 25996–26006. [PubMed: 25078100]

(22). Green MR; Sambrook J How to win the battle with RNase. Cold Spring Harb. Protoc 2019, 2019, pdb.top101857.

(23). Bender AT; Sullivan BP; Lillis L; Posner JD Enzymatic and chemical-based methods to inactivate endogenous blood ribonucleases for nucleic acid diagnostics. J. Mol. Diagn 2020, 22, 1030–1040.

(24). Deindl E; Fischer S; Preissner KT New directions in inflammation and immunity: The multi-functional role of the extracellular RNA/RNase system. Indian J. Biochem. Biophys 2009, 46, 461–466. [PubMed: 20361709]

(25). Lu L; Li J; Moussaoui M; Boix E Immune modulation by human secreted RNases at the extracellular space. Front. Immunol 2018, 9, 1012. [PubMed: 29867984]

(26). Yang D; Chen Q; Rosenberg H; Rybak S; Newton D; Wang Z; Fu Q; Tchernev V; Wang M; Schweitzer B Human ribonuclease A superfamily members, eosinophil-derived neurotoxin and pancreatic ribonuclease, induce dendritic cell maturation and activation. J. Immunol 2004, 173, 6134–6142. [PubMed: 15528350]

(27). Kannemeier C; Shibamiya A; Nakazawa F; Trusheim H; Ruppert C; Markart P; Song Y; Tzima E; Kennerknecht K; Niepmann M; von Bruehl M-L; Sedding D; Massberg S; Günther A; Engelmann B; Preissner KT Extracellular RNA constitutes a natural procoagulant cofactor in blood coagulation. Proc. Natl. Acad. Sci. U. S. A 2007, 104, 6388–6393. [PubMed: 17405864]

(28). Garnett ER; Lomax JE; Mohammed BM; Gailani D; Sheehan JP; Raines RT Phenotype of ribonuclease 1 deficiency in mice. RNA 2018, 25, 921–934.

(29). Dickson KA; Haigis MC; Raines RT Ribonuclease inhibitor: Structure and function. Prog. Nucleic Acid Res. Mol. Biol 2005, 80, 349–374. [PubMed: 16164979]

(30). Thomas SP; Kim E; Kim J-S; Raines RT Knockout of the ribonuclease inhibitor gene leaves human cells vulnerable to secretory ribonucleases. Biochemistry 2016, 55, 6359–6362. [PubMed: 27806571]

(31). Strong LE; Kink JA; Pensinger D; Mei B; Shahan M; Raines RT Efficacy of ribonuclease QBI-139 in combination with standard of care therapies. Cancer Res. 2012, 72 (Suppl. 1), 1838.

(32). Strong LE; Kink JA; Mei B; Shahan MN; Raines RT First in human phase I clinical trial of QBI-139, a human ribonuclease variant, in solid tumors. J. Clin. Oncol 2012, 30 (Suppl.), TPS3113.

(33). Ilinskaya ON; Shah Mahmud R Ribonucleases as antiviral agents. Mol. Biol 2014, 48, 615–623. [PubMed: 32214473]

(34). Chao T-Y; Lavis LD; Raines RT Cellular uptake of ribonuclease A relies on anionic glycans. Biochemistry 2010, 49, 10666–10673. [PubMed: 21062061]

(35). Chao T-Y; Raines RT Mechanism of ribonuclease A endocytosis: Analogies to cell-penetrating peptides. Biochemistry 2011, 50, 8374–8362. [PubMed: 21827164]

(36). Thompson JE; Raines RT Value of general acid–base catalysis to ribonuclease A. J. Am. Chem. Soc 1994, 116, 5467–5468. [PubMed: 21391696]

(37). Lomax JE; Eller CH; Raines RT Comparative functional analysis of ribonuclease 1 homologs: Molecular insights into evolving vertebrate physiology. Biochem. J 2017, 474, 2219–2233. [PubMed: 28495858]

(38). Abel RL; Haigis MC; Park C; Raines RT Fluorescence assay for the binding of ribonuclease A to the ribonuclease inhibitor protein,. Anal. Biochem 2002, 306, 100–107. [PubMed: 12069420]

(39). Haigis MC; Raines RT Secretory ribonucleases are internalized by a dynamin-independent endocytic pathway. J. Cell Sci 2003, 116, 313–324. [PubMed: 12482917]

(40). Johnson RJ; Chao T-Y; Lavis LD; Raines RT Cytotoxic ribonucleases: The dichotomy of Coulombic forces. Biochemistry 2007, 46, 10308–10316. [PubMed: 17705507]

(41). Yan H; Hancock REW Synergistic interactions between mammalian antimicrobial defense peptides. Antimicrob. Agents Chemother 2001, 45, 1558–1560. [PubMed: 11302828]

(42). Wang G; Elliott M; Cogen AL; Exell EL; Gallo RL; Hancock REW Structure, dynamics, and antimicrobial and immune modulatory activities of human LL-23 and its single-residue variants mutated on the basis of homologous primate cathelicidins. Biochemistry 2012, 51, 653–664. [PubMed: 22185690]

(43). Cory AH; Owen TC; Barltrop JA; Cory JG Use of an aqueous soluble tetrazolium/formazan assay for cell growth assays in culture. Cancer Commun. 1991, 3, 207–212. [PubMed: 1867954]

(44). Okumura K; Itoh A; Isogai E; Hirose K; Hosokawa Y; Abiko Y; Shibata T; Hirata M; Isogai H C-Terminal domain of human CAP18 antimicrobial peptide induces apoptosis in oral squamous cell carcinoma SAS-H1 cells. Cancer Lett. 2004, 212, 185–194. [PubMed: 15279899]

(45). Chen X; Niyonsaba F; Ushio H; Okuda D; Nagaoka I; Ikeda S; Okumura K; Ogawa H Synergistic effect of antibacterial agents human β-defensins, cathelicidin LL-37 and lysozyme against *Staphylococcus aureus* and *Escherichia coli*. J. Dermatol. Sci 2005, 40, 123–132. [PubMed: 15963694]

(46). Hollmann A; Martinez M; Maturana P; Semorile LC; Maffia PC Antimicrobial peptides: Interaction with model and biological membranes and synergism with chemical antibiotics. Front. Chem 2018, 6, 204. [PubMed: 29922648]

(47). Prats-Ejarque G; Li J; Ait-Ichou F; Lorente H; Boix E Testing a human antimicrobial RNase chimera against bacterial resistance. Front. Microbiol 2019, 10, 1357. [PubMed: 31275278]

(48). Li JR; Fernández-Millán P; Boix E Synergism between host defence peptides and antibiotics against bacterial infections. Curr. Top. Med. Chem 2020, 20, 1238–1263.

(49). Demchick P; Koch AL The permeability of the wall fabric of *Escherichia coli* and *Bacillus subtilis*. J. Bacteriol 1996, 178, 768–773. [PubMed: 8550511]

(50). Morè N; Martorana AM; Biboy J; Otten C; Winkle M; Gurnani Serrano CK; Montón Silva A; Atkinson L; Yau H; Breukink E; den Blaauwen TWV; Polissi A Peptidoglycan remodeling enables *Escherichia coli* to survive severe outer membrane assembly defect. mBio 2019, 10, e02729–18. [PubMed: 30723128]

(51). Lomax JE; Eller CH; Raines RT Rational design and evaluation of mammalian ribonuclease cytotoxins. Methods Enzymol. 2012, 502, 273–290. [PubMed: 22208989]

(52). Boix E; Salazar VA; Torrent M; Pulido D; Nogués MV; Moussaoui M Structural determinants of the eosinophil cationic protein antimicrobial activity. Biol. Chem 2012, 393, 801–815. [PubMed: 22944682]

(53). Torres MDT; Sothiselvam S; Lu TK; de la Fuente-Nunez C Peptide design principles for antimicrobial applications. J. Mol. Biol 2019, 431, 3547–3567. [PubMed: 30611750]

(54). Parkinson JS; Houts SE Isolation and behavior of *Escherichia coli* deletion mutants lacking chemotaxis functions. J. Bacteriol 1982, 151, 106–113. [PubMed: 7045071]

(55). Sezonov G; Joseleau-Petit D; D'Ari R *Escherichia coli* physiology in Luria–Bertani broth. J. Bacteriol 2007, 23, 8746–8749.

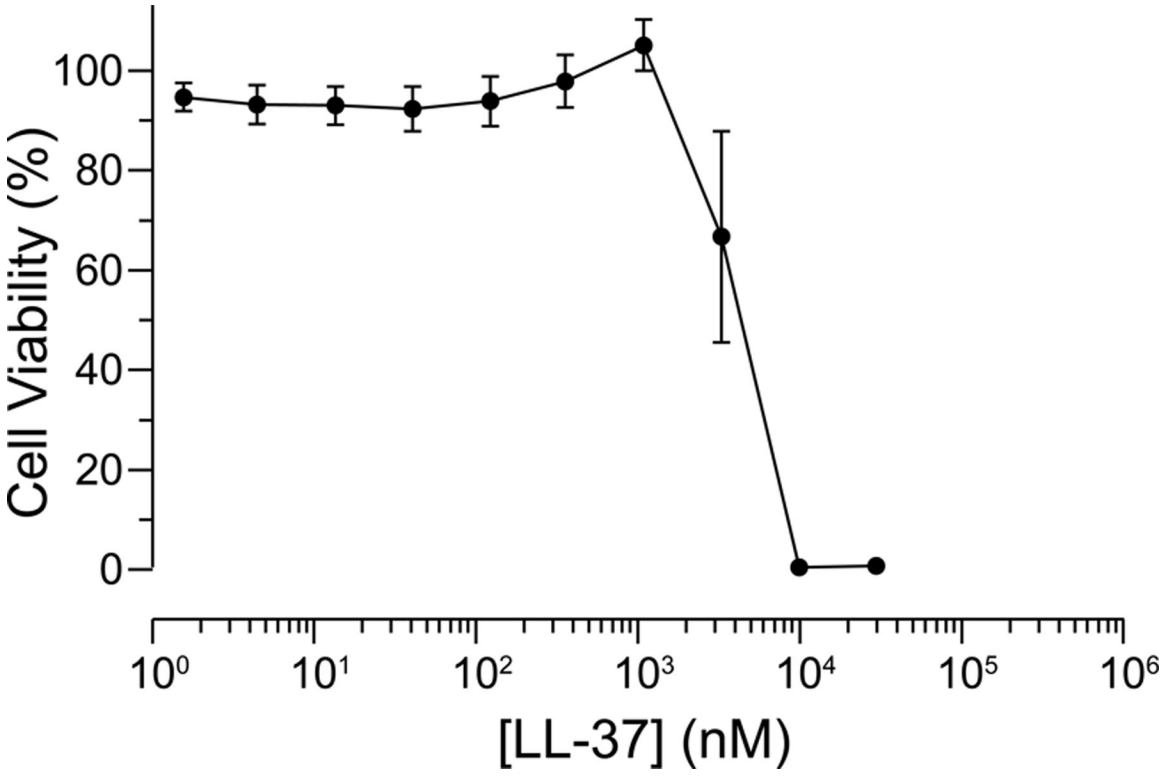


**Figure 1.**

Effect of LL-37 on the viability of *E. coli* cells. Cells were treated with LL-37 for 18 h at 37 °C. Cell viability was assessed via $OD_{600\ nm}$.

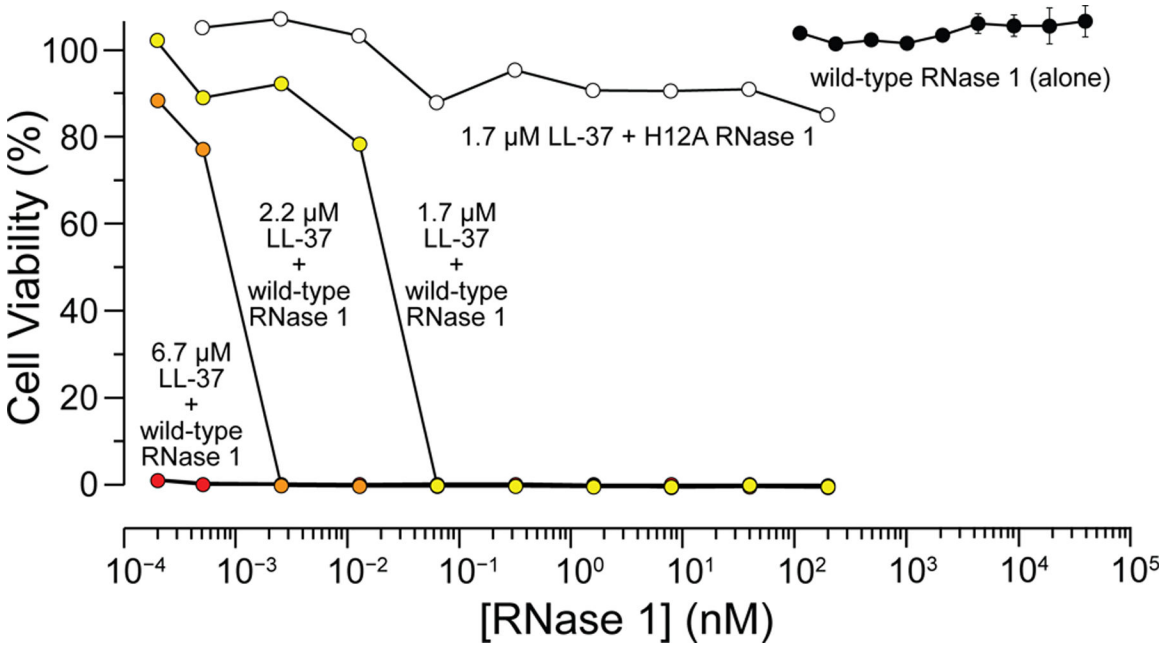


**Figure 2.**

Effect of RNase 1 plus LL-37 on the viability of *E. coli* cells. Cells were treated with the indicated agents for 18 h at 37 °C. Cell viability was assessed via $OD_{600\ nm}$.

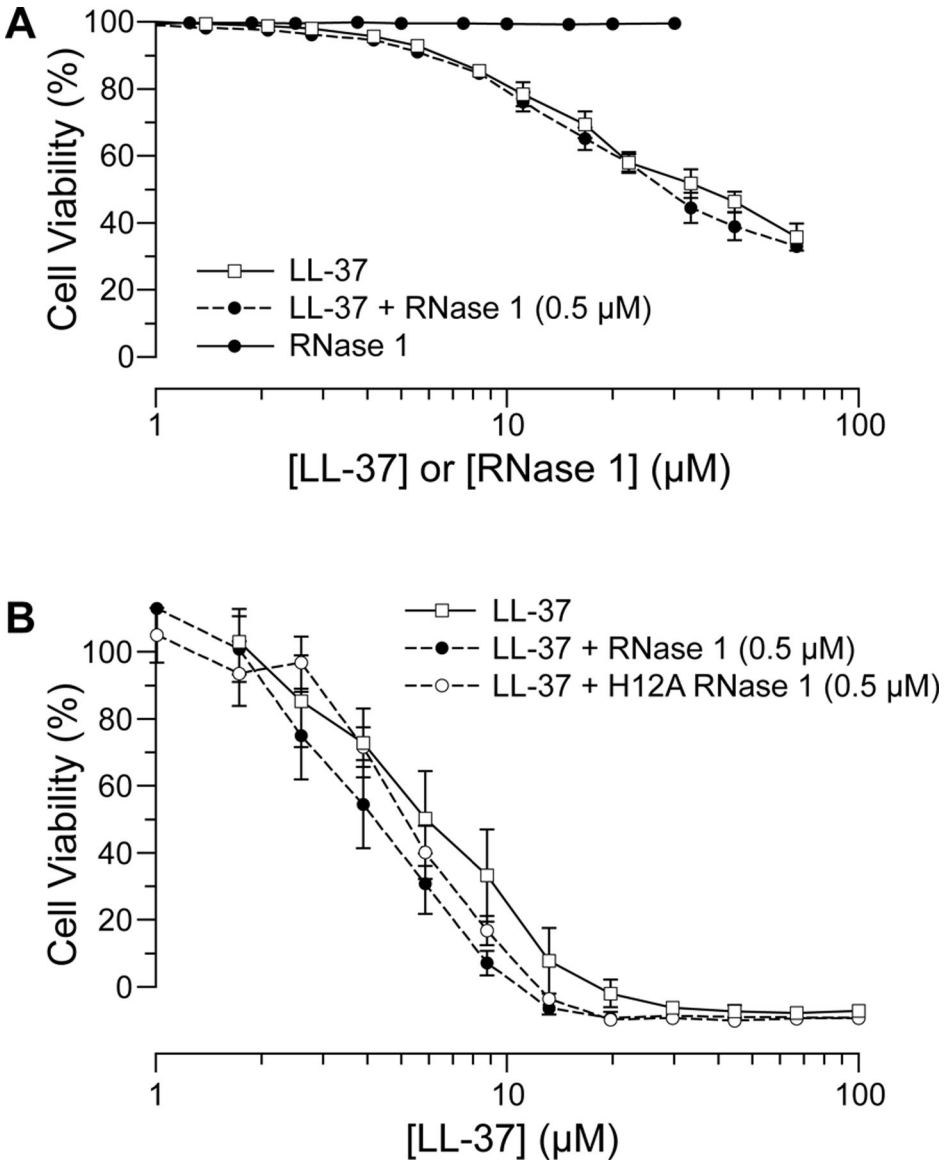


**Figure 3.**

Effect of LL-37 and RNase 1 on the viability of human cells. Cells were treated with a putative toxin. (A) Red blood cells. Cells were treated for 1 h at 37 °C, when the viability was measured by the release of hemoglobin ($A_{405\ nm}$). (B) HUVEC cells. Cells were treated for 24 h at 37 °C, at which time the viability was assessed with a tetrazolium dye-based assay for metabolic activity.[43]

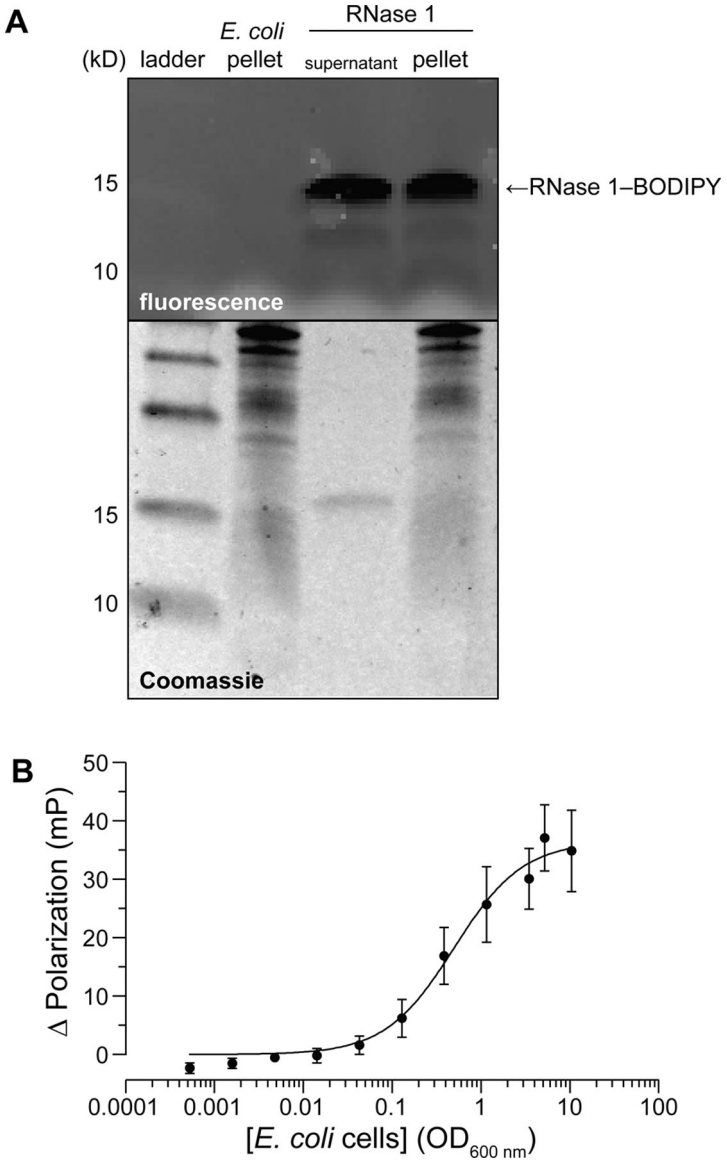


**Figure 4.**

Binding of RNase 1 to *E. coli* cells. (A) SDS–PAGE gel of unbound (supernatant) and bound (pellet) fractions after incubation of RNase 1–BODIPY with *E. coli* cells for 30 min at 37 °C. The gel was imaged by fluorescence (top) or staining with Coomassie Brilliant Blue G-250 dye. (B) Graph showing the fluorescence polarization of RNase 1–BODIPY (50 nM) in the presence of increasing concentrations of *E. coli* cells. Polarization values are relative to that in the absence of *E. coli* cells. $K_d$ = (0.50 ± 0.04)$OD_{600\ nm}$ = (0.40 ± 0.03) × $10^9$ cells/mL.

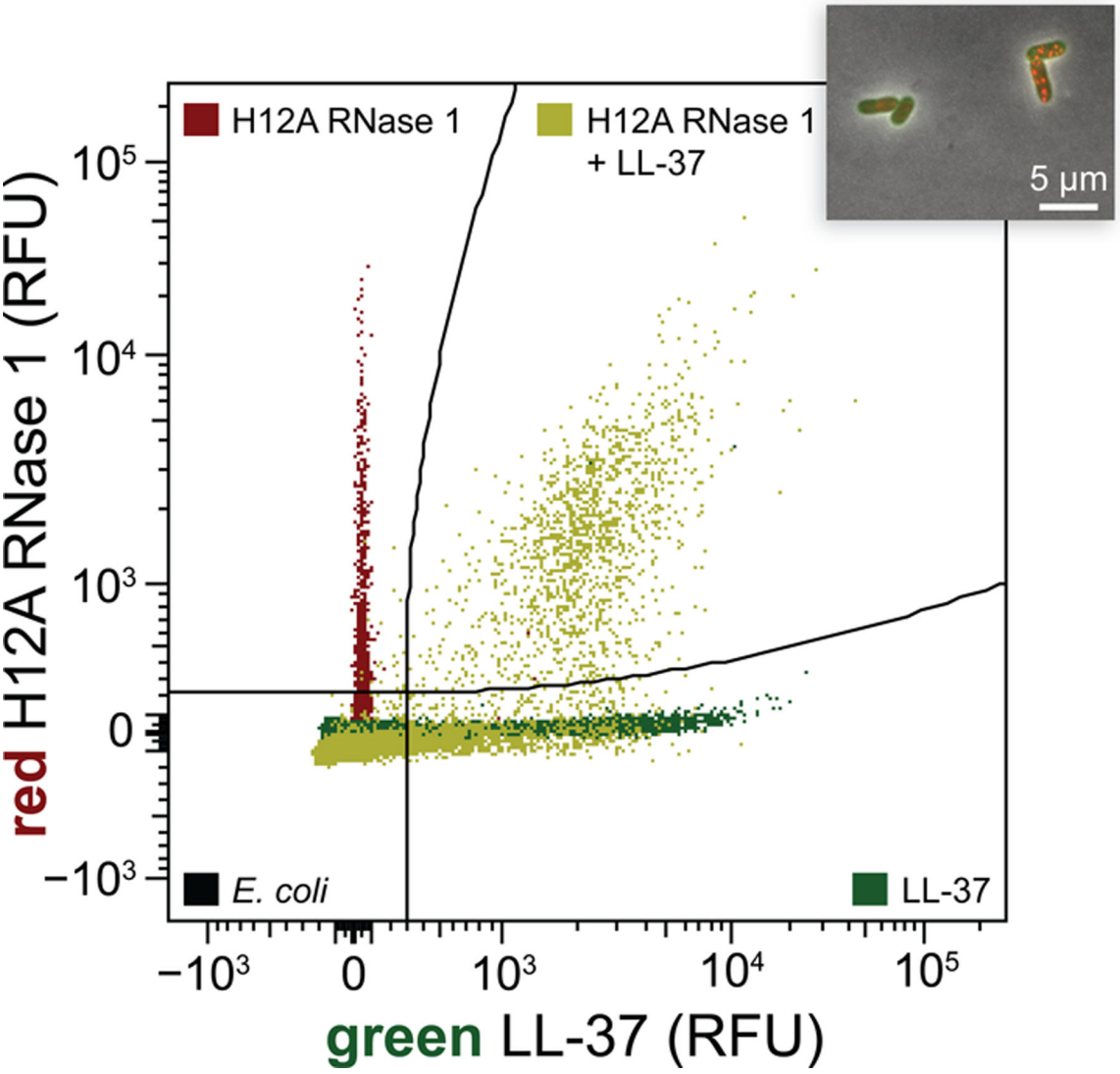


**Figure 5.**

Flow cytogram of *E. coli* cells ($8 \times 10^7$) incubated with 2.5 μM H12A RNase 1–rhodamine (red), 2.5 μM LL-37–BODIPY (green), or both (yellow) in PBS for 2 h. Inset: Confocal microscopy image of *E. coli* cells incubated with H12A RNase 1–rhodamine and LL-37–BODIPY.